Clinical and Translational Imaging (2019) 7:45–60
https://doi.org/10.1007/s40336-018-0307-6

PICTORIAL ESSAY

PET in brain tumors

Davide Donner[1] · Umberto Rozzanigo[2] · Dante Amelio[3] · Silvio Sarubbo[4] · Daniele Scartoni[3] · Lorena Picori[1] · Maurizio Amichetti[3] · Franco Chioffi[4] · Franca Chierichetti[1]

Received: 29 August 2018 / Accepted: 19 November 2018 / Published online: 4 December 2018

Abstract

Purpose The aim of this Pictorial Essay is to illustrate the metabolic aspect of PET (positron emission tomography) imaging in relation to conventional and advanced MR (magnetic resonance) of brain neoplasms.

Materials 10 patients, who performed PET–CT with amino acid tracers and/or FDG were selected from a series of more than 250 cases from a single institution. The selection was made to illustrate and discuss each of the indications reported in the European guidelines. Fusion imaging was obtained merging PET–CT with MR T1-CE (contrast enhanced) and/or T2/FLAIR sequences. The SUV_{max} of the lesion and the SUV_{max} lesion to SUV_{max} background ratio were evaluated. The lesion uptake was also assessed using a five-point visual scale with a range from − 2 to + 2 in relation to basal ganglia uptake. The Hospital Information System (HIS) and the proton therapy data archives have been used for clinical history. For each case, the critical issues were described and the physiopathological correlations were provided to explain the imaging findings.

Conclusions The complexity of illustrated cases demonstrates the need for a multidisciplinary board evaluation to reach a more accurate diagnosis.

Keywords Brain lesions · Differential diagnosis · PET–CT imaging · Advanced MR

Introduction

In Europe, the brain tumors incidence is of 5 cases per 100,000 inhabitants/year, without significant differences between different countries [1].

The new WHO 2016 classification of central nervous system (CNS) tumors use molecular parameters in addition to histology to define tumor entities, defining how CNS tumor diagnoses should be structured in the molecular era [2, 3].

MR is the fundamental imaging technique to study brain lesions with both conventional (T2-weighted images, FLAIR and gadolinium-enhanced T1 weighted) [4] and advanced imaging (diffusion, perfusion and spectroscopy) [5, 6].

✉ Davide Donner
davide.donner@apss.tn.it

[1] Nuclear Medicine Department, Santa Chiara Hospital, APSS Trento, Trento, Italy

[2] Radiology Department, Santa Chiara Hospital, APSS Trento, Trento, Italy

[3] Proton Therapy, APSS Trento, Trento, Italy

[4] Neurosurgery, Santa Chiara Hospital, APSS Trento, Trento, Italy

In clinical practice, the nuclear medicine imaging is increasingly performed to study brain tumors [7] also because MR techniques, even advanced ones, may not always be conclusive, especially in therapy monitoring.

The PET–CT radiopharmaceuticals used in our routine are two AA tracers *O*-(2-[18F] fluoroethyl)-L-tyrosine (^{18}F-FET) and 3,4-dihydroxy-6-18F-fluoro-L-phenylalanine (^{18}F-DOPA) [8] and [18F] 2-fluoro-2-deoxy-D-glucose (^{18}F-FDG) [9].

The absorption of AA-PET tracers in tumor cells is mainly (> 80%) due to LAT L-type amino acid transporter (LAT), which highlights the increased proliferative activity [8]. ^{18}F-FDG uptake of tumor cells, related to expression levels of glucose transporter 1 (GLUT1), can still play a role in the differential diagnosis and grading of malignant neoplasms, although the physiological uptake of the cerebral cortex and the overlap with some benign lesions may represent a limit [9, 10].

The purpose of this iconographic collection is to illustrate the metabolic patterns (^{18}F-FDG, ^{18}F-DOPA and ^{18}F-FET uptake) of primitive brain tumors and the corresponding conventional and advanced MR imaging.

The common clinical indications for PET imaging in brain tumors, as reported in the new International Guidelines [10], are the following: (1) primary diagnosis [11], (2) differential diagnosis of tumor recurrence/radiotherapy planning [12, 13], and (3) disease and therapy monitoring [13].

From a series of over 250 patients, from a single center, a total of 10 cases were selected and arranged according to the above three subgroups of indications. For each case, a variety of specific difficulties in imaging interpretation are discussed, trying to provide, at the end of each one, a physiopathological explanation.

Case histories

CASE 1: suspicion of high-grade glioma

A 50-year-old woman with loss of consciousness due to complex partial epilepsy at onset, with mild left hemiparesis, underwent conventional MRI that revealed a cortical–subcortical lesion in the right middle frontal gyrus, characterized by signal hyperintensity in Fluid-Attenuated Inversion Recovery (FLAIR) images (diameter of 3 cm), without microbleeds in the T2* GRE (Gradient Echo) sequence, with small ring-like areas of T1-CE after gadolinium administration.

Advanced MR: the diffusion was not restricted in Apparent Diffusion Coefficient (ADC) map at the level of this lesion, but the Perfusion-Weighted Imaging (PWI) showed a small area of neoangiogenesis with relative Cerebral Blood Volume (rCBV) > 2. Single-voxel MR spectroscopy (MRS) showed an inversion of the Cho/NAA ratio that was suggestive of a High-Grade Glioma (HGG).

A dynamic ^{18}F-FET-PET, according to current International Guidelines (RANO/EANO/EANM Practice Guideline/SNMMI), was performed. The PET images were fused with T1-CE MR sequences confirming that the whole lesion, not only the small enhancing foci, was highly hypercellular (SUV_{max} lesion = 5.5) with an early peak after 5 min in the dynamic acquisition and a decreasing slope of time/activity curve, compatible with a HGG [14, 15].

After total lesion excision, the histopathological analysis showed a grade IV GBM (glioblastoma), MGMT methylated [promoter methylation status of the gene encoding for the repair enzyme *O*-6-methylguanine DNA methyltransferase], IDH1 wild type [isocitrate dehydrogenase 1], 1p19q co-deletion negative. Radiotherapy and adjuvant chemotherapy have been performed and now the disease-free survival is 2 years (Fig. 1).

Keynotes

AA-PET was useful to confirm the MR suspicion of GBM because some MR features (absence of microhaemorrhages, no restriction of the diffusion, no intratumoral necrosis) were not indicative of a high-grade tumor.

The Time To Peak (TTP) < 12.5 min detected is an index of a worse Overall Survival (OS) and Progression-Free Survival (PFS), compared with a TTP higher than 12.5 min [14, 16].

^{18}F-FET PET has also been useful for surgical planning, to assess the lesion extent to be resected with greater accuracy than the T1-CE MR.

CASE 2: inflammatory lesion versus glioma

A 53-year-old man, in pharmacological coma for generalized tonic–clonic seizures, whose MR imaging detected an area of FLAIR hyperintensity and cortical swelling in the left parietal lobe, without hemosiderin deposition in T2*GRE, surrounding a superficial 1-cm nodule characterized by restricted diffusion evident in DWI (Diffusion-Weighted Imaging) and ADC map.

After paramagnetic contrast administration this nodule demonstrated poor enhancement and low increase of the perfusion parameter (rCBV < 2). MR spectroscopy (single-voxel; short echo time [TE]) at this level detected a peak of Myoinositol (glial marker not specific for glioma), but not inversion of Cho/NAA. The advanced and conventional MRs were not conclusive.

^{18}F-FDG-PET was performed to exclude an inflammatory lesion. PET images fused with T2 images showed global hypometabolism of left parietal lobe. Further investigation with ^{18}F-DOPA-PET demonstrated a focal light tracer uptake ($SUV_{max} = 1$) corresponding to the MR restricted diffusion nodule (sign of hypercellularity) [17, 18].

The patient was initially treated with high-dose steroids because neurologists suspected an inflammatory/paraneoplastic lesion based on the finding of oligoclonal bands in cerebrospinal fluid (CSF) and positive serum anti-Yo antibodies, but the lesion remained unchanged at control MR performed 2 months later.

A biopsy of the nodule for extemporaneous histological examination and contextual removal of the entire hyperintense lesion in FLAIR were performed by neurosurgeons.

Histopathological data showed an anaplastic astrocytoma grade III WHO (MGMT promoter not methylated, IDH wild type, immuno-reactivity positive for GFAP [Glial Fibrillary Acidic Protein], P53 [< 5%] and Ki67/MIB1 [40%]). The highest grading was found only in the central nodule above described. A chemo-radiotherapy cycle is ongoing (Fig. 2).

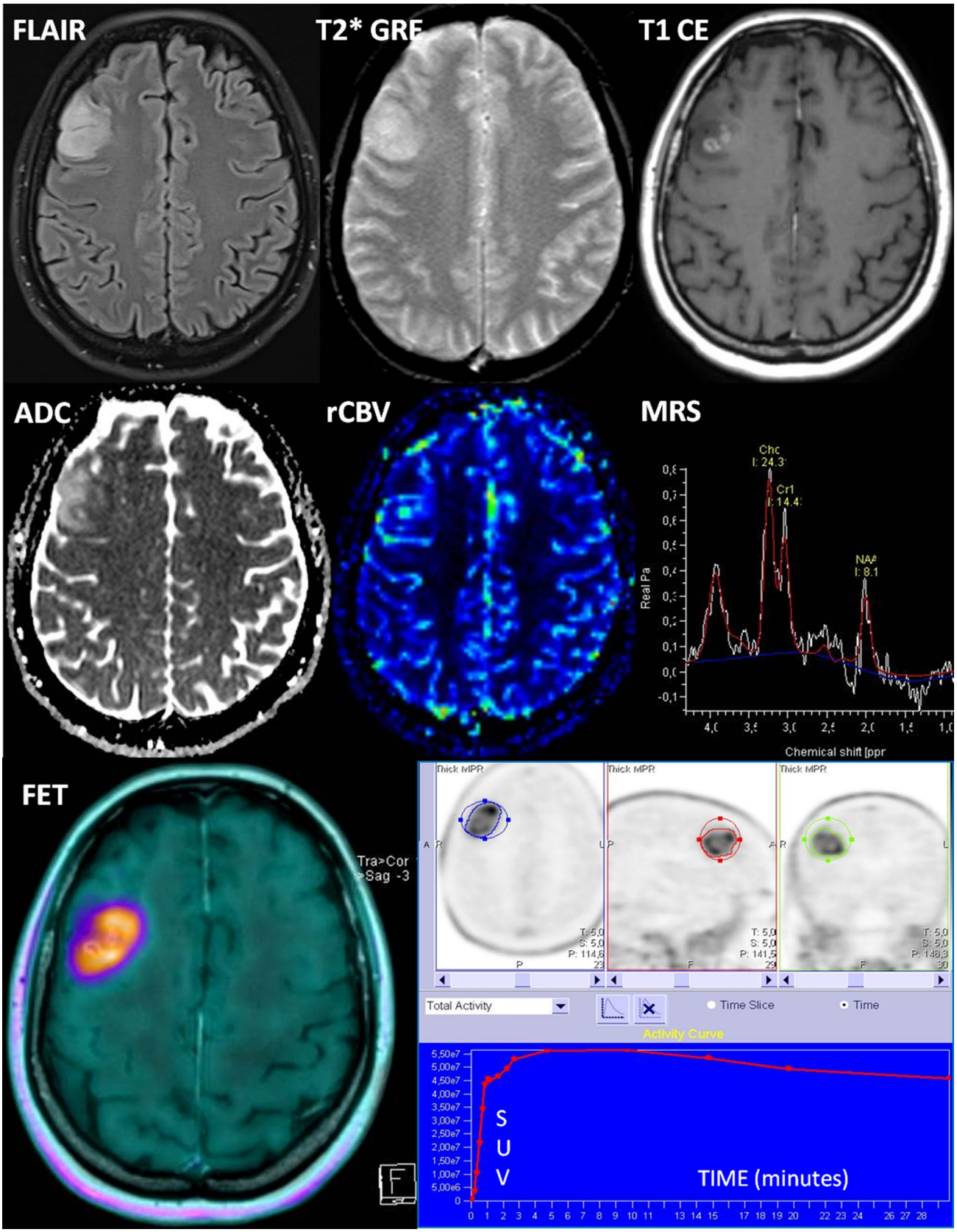

Fig. 1 High-grade glioma

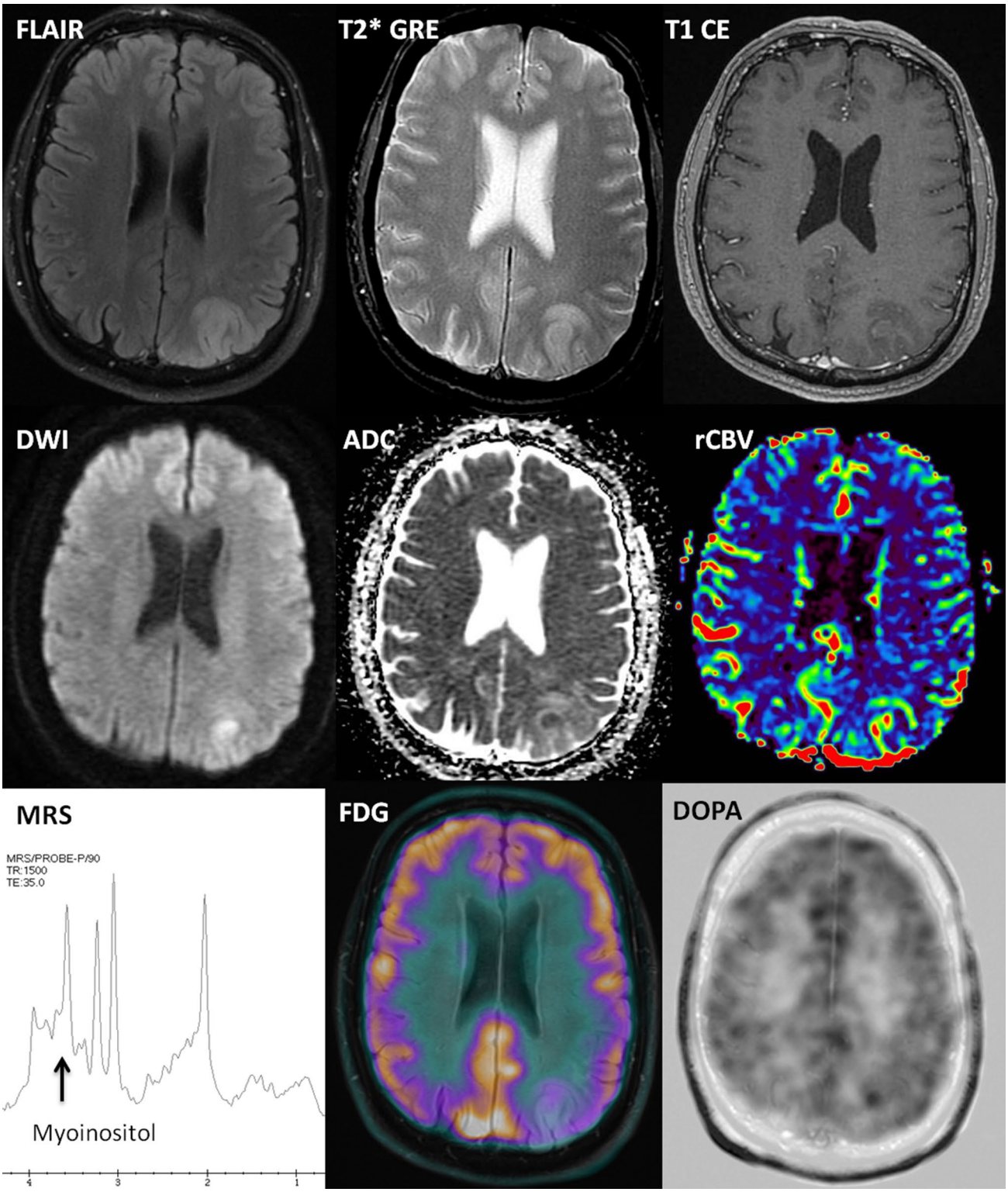

Fig. 2 Anaplastic astrocytoma grade III WHO

Keynotes

^{18}F-DOPA-PET exam was useful in this case to locate the target for biopsy [19], whereas negative ^{18}F-FDG-PET allowed to exclude an inflammatory lesion in active phase.

CASE 3: HGG vs primitive cerebral lymphoma

A 60-year-old man was admitted in coma and metabolic acidosis in intensive care unit. Initial plain CT detected a hyperdense subcortical right frontal lesion with a hypodense necrotic core, surrounded by a wide area of perilesional edema, as evident in the FLAIR image. High-dose corticosteroid therapy was started suspecting HGG. MR examination 2 days later showed initial shrinkage (from 3 to 2.3 cm) of the solid portion of the formation, characterized by marked restricted diffusion in DWI/ADC maps and by ring contrast enhancement in T1-w sequence. The lesion appeared hypovascular at perfusion imaging, with low rCBV values, opposite to what was expected in case of HGG. MR spectroscopy (MRS) demonstrated elevated lipid-lactate peaks in the spectral analysis (single-voxel, short-TE technique) and inversion of Cho/NAA ratio, better seen in the metabolite map obtained with MRS multivoxel intermediate TE technique.

The suspicion of a primary central nervous system lymphoma (PCNSL) instead of a HGG was suggested by the mismatch between the highly aggressive MRS pattern and the low rCBV perfusion values (despite contrast enhancement), associated with lesion diffusion restriction and imaging response to steroid therapy.

PCNSL, high-grade glioma and brain metastases are all examples of common enhancing malignant brain tumors on MR, but this lesion showed low values in perfusion imaging (rCBV < 2), because the enhancement in lymphoma is due to barrier damage rather than to neoangiogenesis, which characterizes high-grade gliomas (rCBV > 2). The PCNSL spectral analysis may be similar to that of HGG, with an inversion of the Cho/NAA ratio and a lipid peak, since, as in this case, a necrotic center was also present.

Cerebral PET imaging with ^{18}F-DOPA and ^{18}F-FDG was, therefore, performed about 2 weeks after admission and fused with MR T1-CE sequence: the frontal lesion was further shrunken, but there was intense focal uptake of both tracers (^{18}F-FDG: SUV_{max} lesion = 18.3, SUV_{max} background = 8.2 and SUV_{max} lesion to SUV_{max} background ratio = 2.23; ^{18}F-DOPA: SUV_{max} lesion max = 2.5, SUV_{max} background = 0.7 and SUV_{max} lesion to SUV_{max} background ratio = 3.6). The staging CT scan performed was negative. Brain biopsy documented non-Hodgkin B-cell primary CNS lymphoma. Chemotherapy was performed with good response for 2 years and subsequent recurrence and death (Fig. 3).

Keynotes

Cerebral lymphoma is generally characterized by very high ^{18}F-FDG tracer focal uptake ($SUV_{max} \gg 4$) values [20, 21] that can help to consider the diagnosis of this type of pathology compared to other lesions such as high-grade gliomas or metastases that may be hypermetabolic [22, 23].

The high-lesion ^{18}F-DOPA uptake detected, in this case, leads us to hypothesize that also lymphoma cells can be characterized by an overexpression of LAT 1 (L-type amino acid transporter) and cofactor CD98 [24]. This feature could be useful in staging of PCNSL that can affect any part of the neuraxis, including the eyes, brain, leptomeninges, or spinal cord.

CASE 4: suspect LGG vs malformation of cortical development

A 52-year-old man with partial epileptic seizures secondarily generalized, with olfactory hallucinations (uncinate crisis) underwent conventional MR that revealed thickening of the left parahippocampal cortex in the coronal T1-IR (Inversion Recovery) with blurring of white matter–gray matter junction, associated with mild increased T2/FLAIR signal of the left temporo-mesial region, involving the amygdala and the uncus, without contrast enhancement: a tumefactive Low-Grade Glioma (LGG) was initially suspected. Advanced MR (not shown) was negative: diffusion imaging was normal, perfusion rCBv value was not increased, and single-voxel spectral analysis was symmetric with the contralateral side, without pathological changes.

^{18}F-DOPA-PET brain examination showed no significant uptake in the left tempo-mesial region (see fusion with FLAIR image), excluding the initial hypothesis of a LGG. ^{18}F-FDG-PET imaging was performed to rule out limbic encephalitis due to paraneoplastic syndrome, whole body scan was negative for tumors, and the brain study demonstrated bilateral symmetric hypometabolism of the temporo-mesial regions (see fusion with T2-w image).

Follow-up with serial MR every 3 months during 1 year showed no morphologic or signal changes in the left temporo-mesial region. All the laboratory tests (inflammatory, infective and neoplastic markers) were negative. The patient responded to antiepileptic drugs without the need for neurosurgery for refractory epilepsy. The final diagnosis was adult-onset focal cortical dysplasia (Fig. 4).

Keynotes

The absence of pathological AA tracer uptake is important to exclude with reasonable certainty the presence of a LLG, which sometimes can be associated with focal

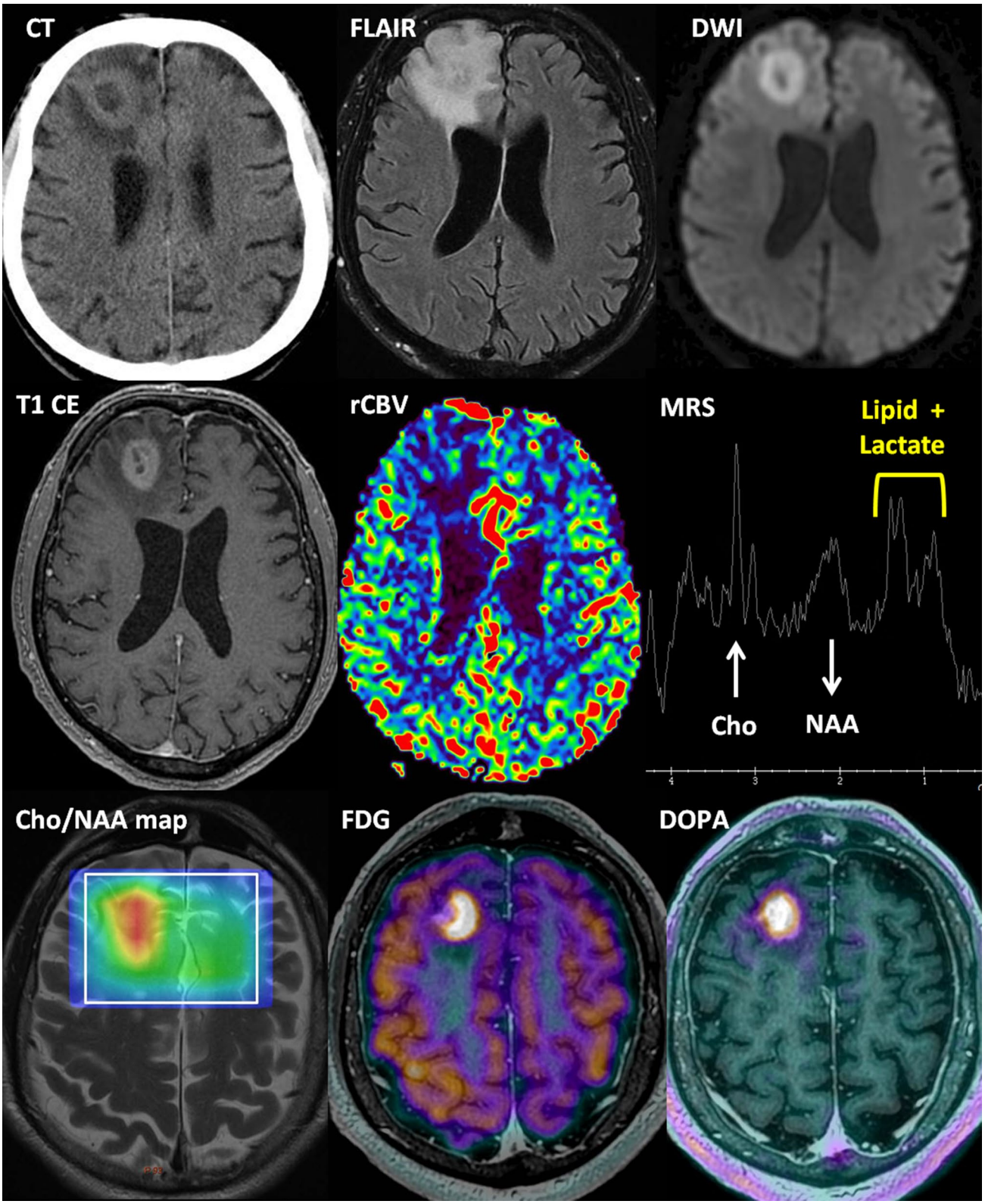

Fig. 3 Primary central nervous system lymphoma (PCNSL)

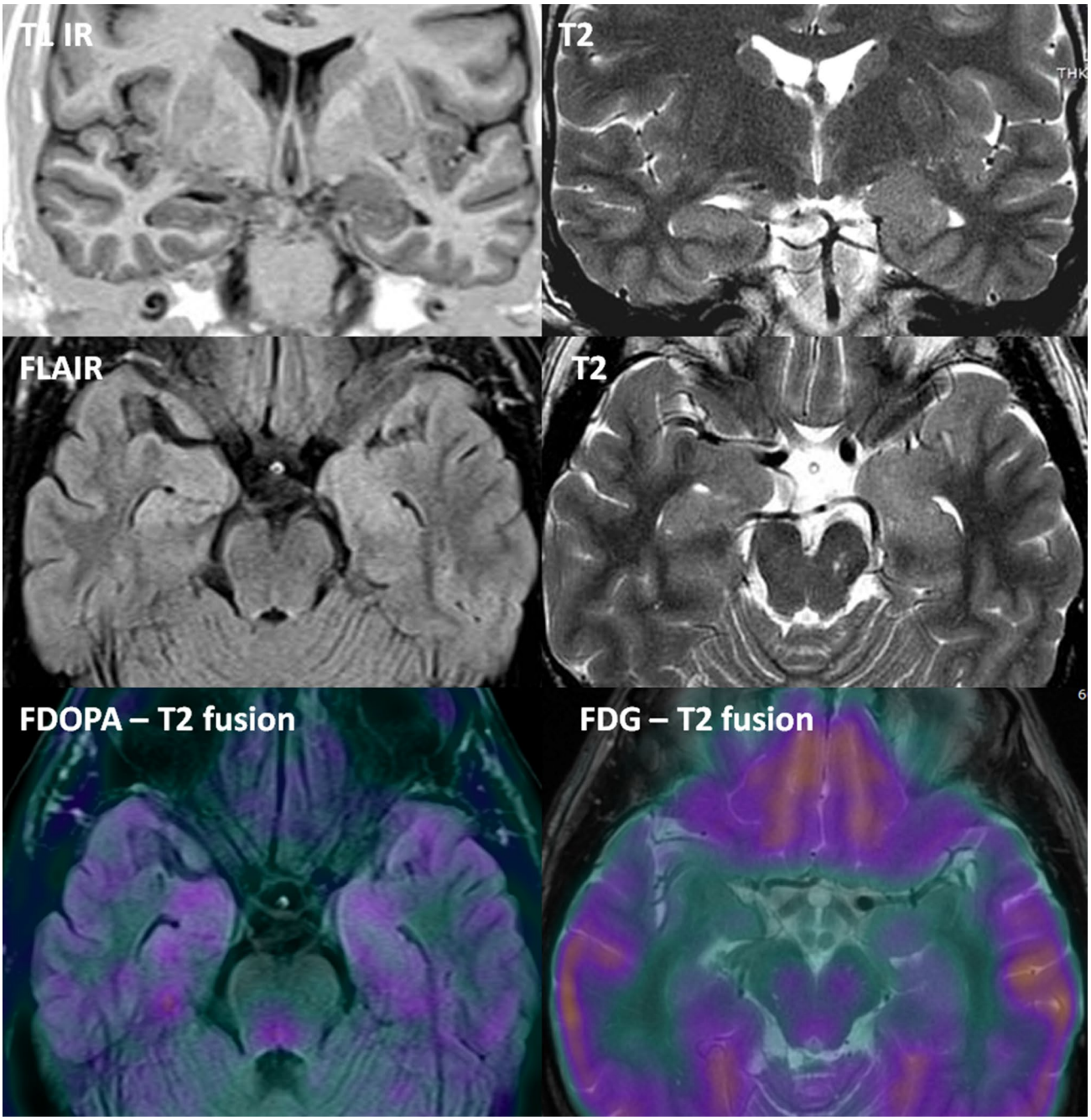

Fig. 4 Focal cortical dysplasia (FCD)

cortical dysplasia (so-called "double pathology") especially when MR is not conclusive [11, 25].

The usefulness of cerebral PET with FDG tracer is to detect inflammatory/infectious forms in the acute phase (typically limbic encephalitis in the temporal lobe) [26]. In this case, ^{18}F-DOPA-PET has been considered a true negative for LGG diagnosis.

CASE 5: residual disease, post-neurosurgery

A 47-year-old man with anaplastic astrocytoma Grade III WHO, MGMT promoter unmethylated [(O86)-methylguanine DNA methyltransferase] and positive IDH1 mutation [isocitrate dehydrogenase 1], P53 (80%) and Ki67/MIB1 (<5%).

MR and ^{18}F-DOPA-PET were performed 1 month after neurosurgery (partial tumor resection), to evaluate the real disease extent for proton therapy planning, that was proposed considering the patient's age and tumor's site which, thanks to the intrinsic dose-saving technique, has the potential advantage of reducing acute and late side effects.

The ^{18}F-DOPA-PET imaging was fused with T1-CE and T2/FLAIR MR sequences that shown a high radiotracer uptake all around the surgical crater in the right frontal lobe, with a relatively higher extension in the anterior part of the same, corresponding to the extent of the hyperintense signal in T2 images and larger than the enhancing tissue [13, 27].

Furthermore, tracer uptake confirmed the suspicion of persistent disease in the contralateral frontal lobe and the involvement of right caudate head (SUV_{max} of right caudate head = 2.2 vs 1.6 of the left caudate head, Delta SUV_{max} right–left = 20–25%). The tumor to background ratio was 2.5.

Proton therapy (60 Gy in 30 fractions) was then performed 1 month after surgery using also the ^{18}F-DOPA-PET data for the radiation treatment planning process. Up to now the patient is still alive (Fig. 5).

Keynotes

^{18}F-DOPA PET fused with T1 and T2 MR sequences allows to confirm the suspicion of residual tumor, improving accuracy of radiotherapy target volume delineation, defining Biological Target Volume (BTV) and consequently modifying Gross Target Volume (GTV) [19, 27].

CASE 6: multifocal disease

A 58-year-old man with multicentric glioblastoma grade IV WHO, IDH1 wt (wild type) and MGMT methylated, underwent neurosurgical intervention in left frontal lobe, followed by photon radiotherapy and concomitant chemotherapy and sequential chemotherapy with temozolomide (75 mg/m^2/die 7 days/week) both for frontal and occipital lesions.

After 9 months, MR pointed out tumor progression in the occipital lobe and the patient received surgical excision at this site. MR and ^{18}F-DOPA-PET were performed to evaluate the extent of residual disease, for possible proton radiotherapy re-irradiation [19].

Conventional MR revealed hyperintense FLAIR areas in left frontal lobe and in right parieto-occipital lobe surrounding the surgical crater, with some foci of T1 contrast enhancement. The data were suspicious for residual disease [28].

The ^{18}F-DOPA-PET fused with T2/FLAIR and T1-CE MR images, documented a high uptake (visual score 0) in left fronto-temporal cortex and in right occipital and calcarine cortex, greater than the extension of the areas of contrast enhanced in T1-weighted images and smaller than the hyperintense areas on T2-weighted FLAIR MR sequences. The ^{18}F-DOPA uptake degree in the calcarine region was higher than the basal ganglia (striatum) uptake (visual score + 1); in the others sites the ^{18}F-DOPA uptake degree was equal to the basal ganglia uptake (visual score 0) [29].

The patient has been successfully treated with proton therapy re-irradiation and concomitant temozolomide (Fig. 6).

Keynotes

^{18}F-DOPA-PET examinations are useful to differentiate radionecrosis vs post-surgery BBB permeability alterations and recurrent disease even in case of already treated patients [29].

CASE 7: therapy monitoring in progression from LGG to HGG

A 74-year-old woman had neurosurgery (partial excision of left frontal lobe tumor lesion) resulting in LGG (gemistocytic astrocytoma II grade WHO, MGMT methylated and IDH1 mutated, in left frontal lobe) followed by radio–chemotherapy.

The planning with conventional MR showed an area of altered FLAIR signal in the left frontal lobe with hemosiderinic deposits at the margins of the surgical crater. After administration of paramagnetic contrast agent, an enhancement area of about 2 cm was detected posterior to the surgical site in the T1-w sequences, suspect for recurrence/disease progression.

Then a ^{18}F-DOPA-PET was performed and fused with T1-CE MR images, which documented a large area of inhomogeneous high tracer uptake involving the brain tissue adjacent to the surgical cavity of left frontal lobe.

The ^{18}F-FDG-PET, also performed in suspicion of an upgrade of the primary tumor, fused with T1-CE MR images, showed a focal high tracer uptake area corresponding to the area of increased rCBV values in recent MR.

^{18}F-FDG detected a global hypometabolism of the extralesional cortex and basal ganglia of the same side with crossed cerebellar diaschisis.

The advanced MRI revealed, in perfusion-weighted imaging (PWI), an increased vascularization in the enhancing nodule posterior to surgical crater, which was associated with an increase in rCBV values also of the more cranial lesion component (index of hyperperfusion), characterized by a moderate restriction of diffusion (DWI hyperintense), related to hypercellularity, but lacking in contrast enhancement.

The enhancing focus with hyperperfusion and hypercellularity was consistent with the focal high uptake of ^{18}F-FDG

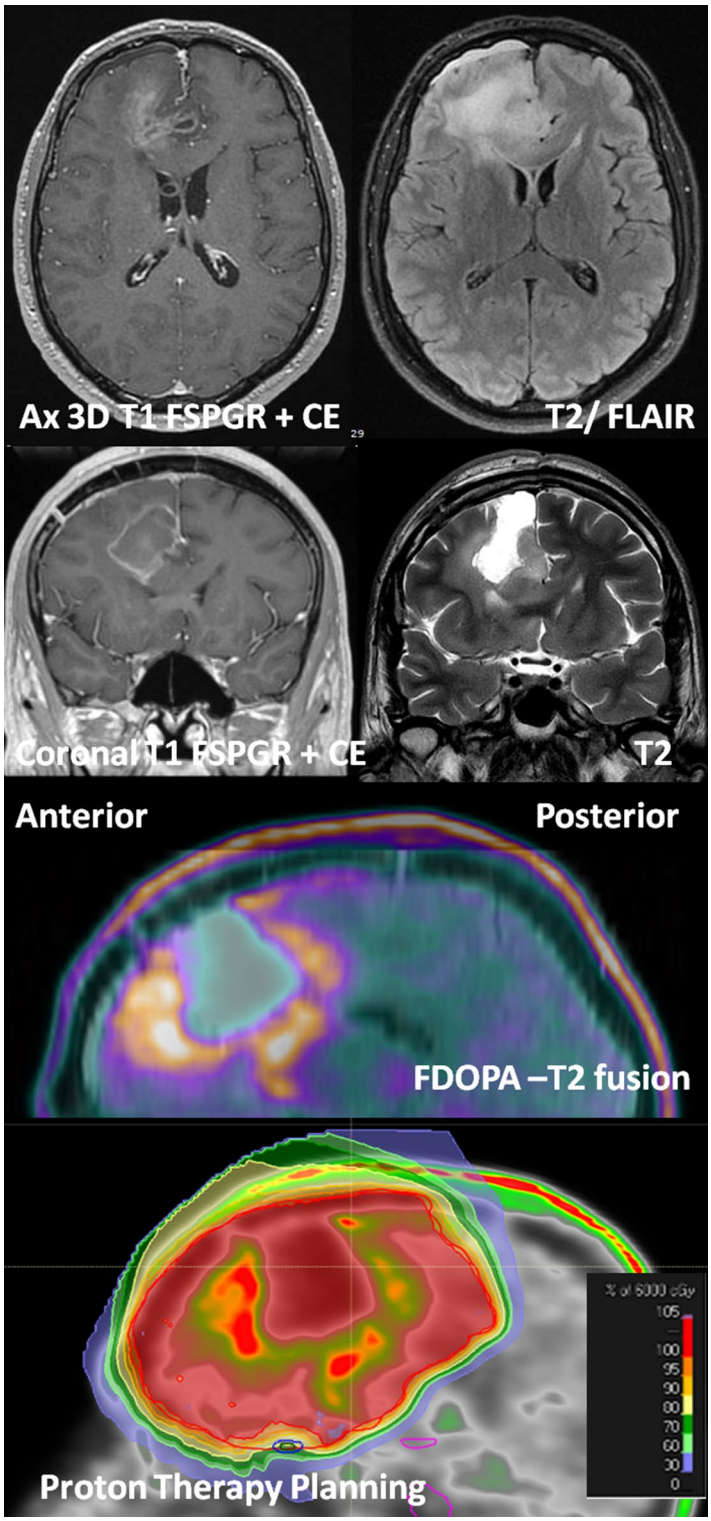

Fig. 5 Residual disease after neurosurgery

and the hyperperfused, hypercellular but not enhancing inT1 sequences, with the relatively higher ^{18}F-DOPA uptake, both studies suggestive for two foci of high-grade neoplasia [30, 31].

After MR and PET evaluation, the data were used to radiotherapy target volume delineation for proton therapy. The patient has been submitted to proton therapy with concomitant chemotherapy with temozolomide.

^{18}F-DOPA-PET at 4, 6 and 12 months to assess response at radio–chemotherapy showed a marked and progressive decrease of tracer uptake volume (volume delta after 6 months = – 40%; volume delta after 12 months = – 48%;

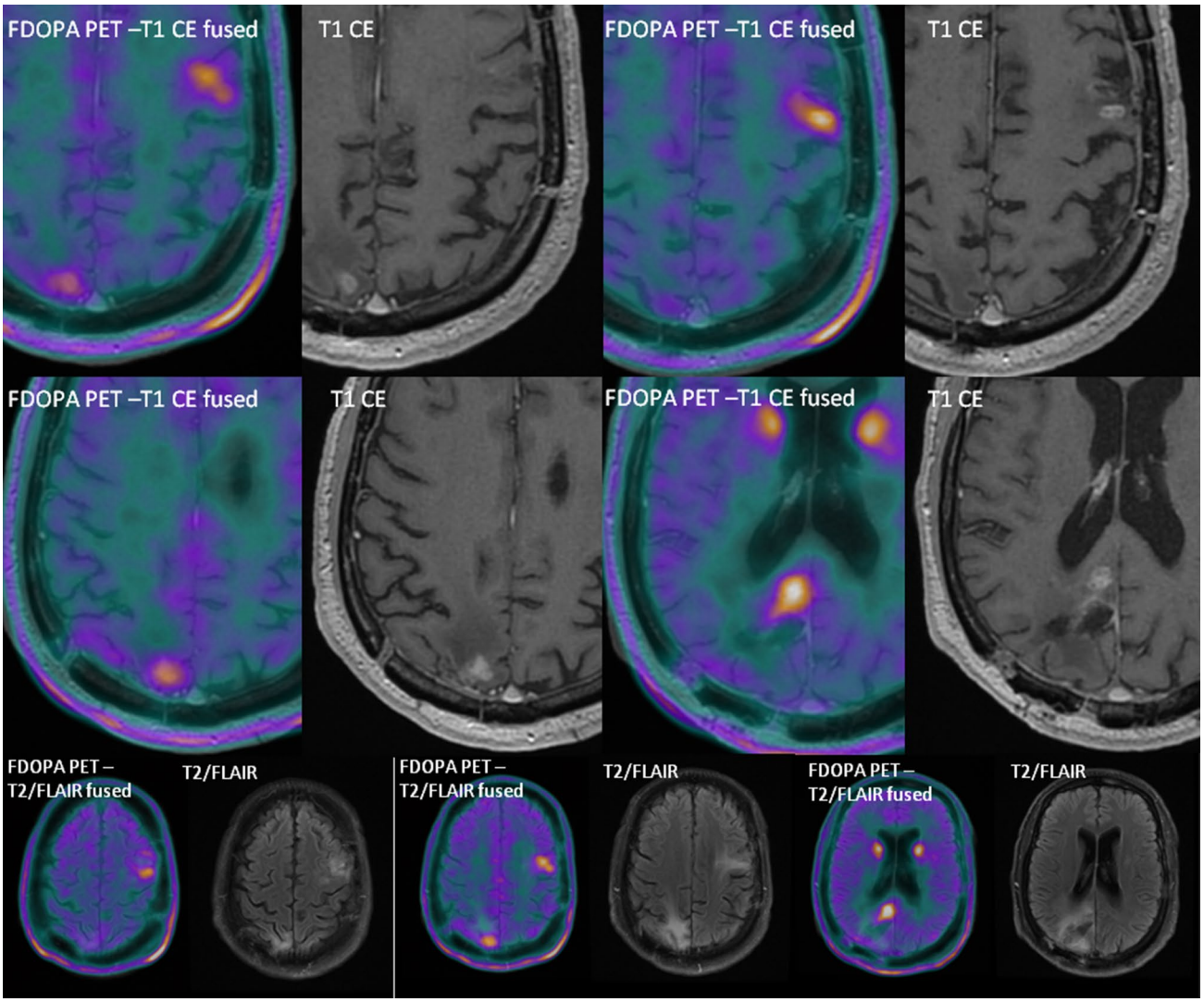

Fig. 6 Multicentric GBM grade IV WHO recurrence

volume delta from 6 to 12 months = − 14%) and a less intense decrease of the tumor to background ratio (SUV_{max} lesion/SUV_{max} background). Nowadays, the disease is stable. Follow-up MR findings were stable and the patient is still alive (Fig. 7).

Keynotes

^{18}F-DOPA and ^{18}F-FDG correctly assess the upgrade of LGG to HGG.

^{18}F-DOPA-PET is particularly useful to detect metabolic changes during and after radiotherapy [8, 30].

CASE 8: LGG recurrence close to basal ganglia

A 34-year-old man, hemophilic, with a diagnosis, 4 years before, of astrocytoma grade II WHO, IDH1 mutated and 1p19q non-codeleted in left temporo-insular region. The MR monitoring performed for 4 years after partial resection surgery showed a slow progressive lesion growth. A second partial resection was performed.

A conventional MR and ^{18}F-DOPA-PET were performed for proton radiotherapy planning because of the hematological pathology. The ^{18}F-DOPA images were fused with T1-CE and T2/FLAIR sequences. The ^{18}F-DOPA showed slight, inhomogeneous radiopharmaceutical uptake (SUV_{max} 1.1) to the left temporal pole, without involvement of insular region and the basal ganglia. ^{18}F-DOPA-PET was acquired using the same thermoplastic mask used for radiotherapy treatment.

24 months after proton therapy, conventional MR revealed a distant recurrence in left posterior para-trigonal site hyperintense in T2-w images, with peripheral contrast

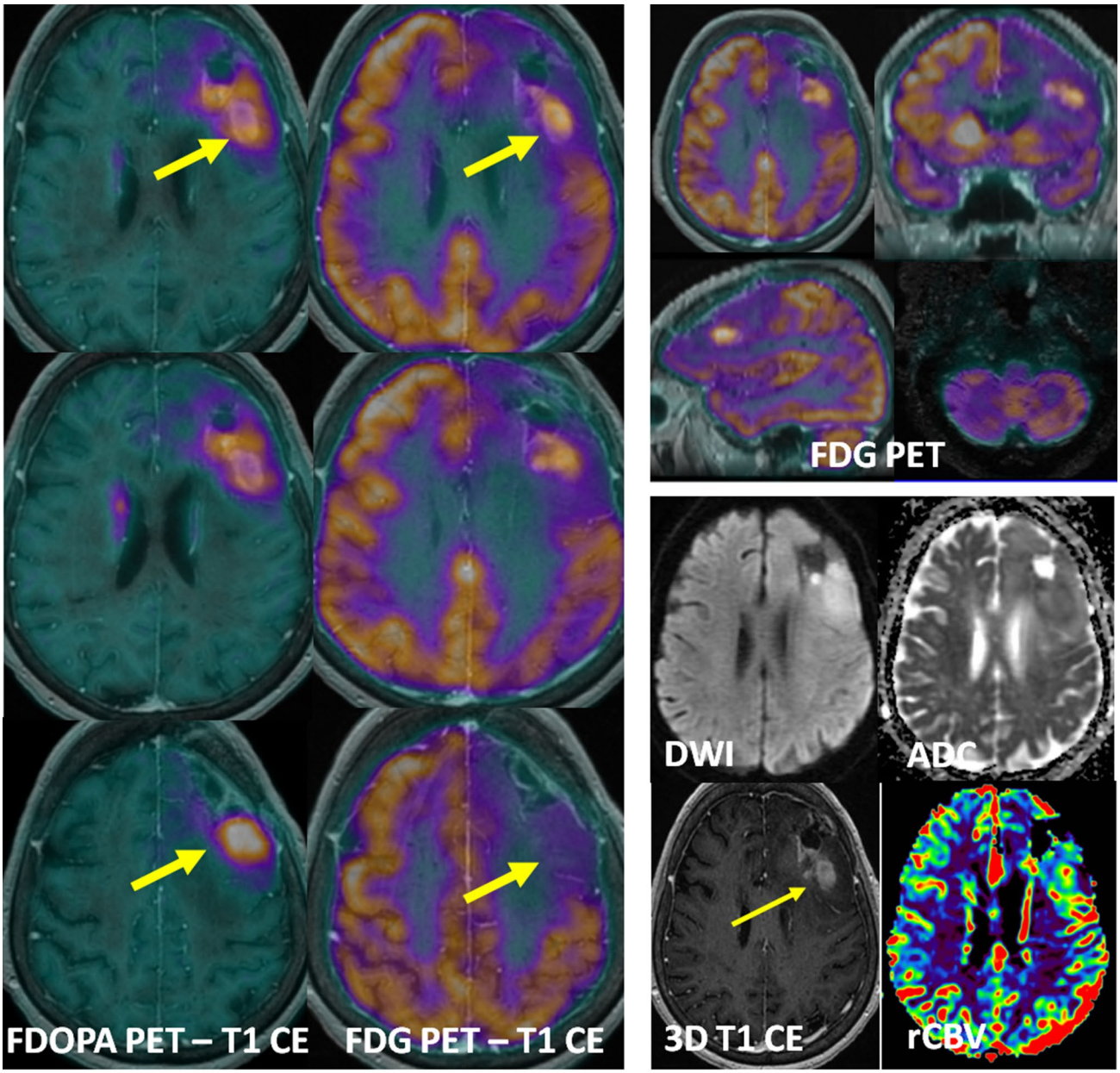

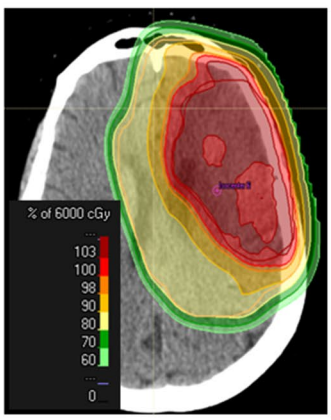

SUV TUMOR	Max 6,14 SUV Min 2,46 SUV Avg. 3,38 SUV Std. Dev. 0,80 Vol. 20,16 cm³	Max 3,67 SUV Min 1,47 SUV Avg. 2,01 SUV Std. Dev. 0,43 Vol. 12,15 cm³	Max 3,27 SUV Min 1,47 SUV Avg. 1,96 SUV Std. Dev. 0,36 Vol. 10,57 cm³
MIP	4 months after surgery	6 months after Protontherapy and Temozolomide	12 months after Protontherapy and Temozolomide
SUV BKG	Max 1,36 SUV	Max 1,04 SUV	Max 0,96 SUV

Fig. 7 FDG and FDOPA PET assessment of disease progression from LGG to HGG after surgery and F-DOPA-PET monitoring response to chemotherapy and radiotherapy

enhancement in T1-w sequences, without increased rCBV values (hypo-vascularization).

^{18}F-FET-PET was preferred to ^{18}F-DOPA-PET to assess residual lesion considering the risk of basal ganglia involvement.

^{18}F-FET-PET showed a moderate tracer uptake (SUV_{max} lesion/SUV_{max} background = 1.5) in the left para-trigonal area and also a lower uptake in the homolateral putamen (arrows), both consistent with recurrent disease, but less extensive with respect to MR findings (Fig. 8).

Keynotes

The use of ^{18}F-FET-PET is mandatory in patients with suspected recurrence or disease progression involving the basal ganglia; although different tracers were used before and after radiotherapy in this case, both examinations provided useful information in different phases of therapy management [32, 33].

CASE 9: disease progression vs radionecrosis

A 35-year-old man was operated for a right frontal LGG with diagnosis of diffuse astrocytoma grade II WHO. After 13 months of follow-up, MR suspected disease progression

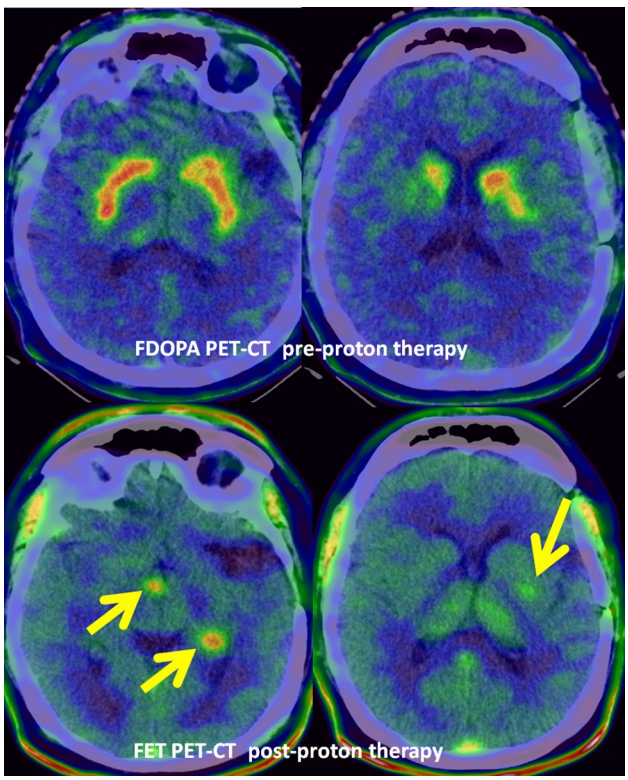

Fig. 8 F-DOPA and FET-PET in LGG recurrence close to basal ganglia

because of the appearance of some small foci of CE in the context of the T2/FLAIR altered signal area close to the surgical crater.

The ^{18}F-DOPA-PET examination showed, in frontal para-median region, an irregular tracer hyper-concentration involving the posterior margin of the surgical cavity, with greater uptake gradient on the mesial side.

^{18}F-FDG-PET was also performed because of the ^{18}F-DOPA uptake gradient (visual score + 2) and of doubtful MR features.

The ^{18}F-FDG-PET documented absence of significant radiopharmaceutical uptake at the posterior margin of surgical cavity. ^{18}F-DOPA (high uptake) and ^{18}F-FDG (hypometabolism) PET–CT were consistent with persistent LGG. Contrast-enhancing pattern was consistent with upgrade and proton therapy treatment was performed (60 Gy RBE in 30 sessions).

17 months after due to new contrast-enhancing areas to exclude tumor progression after proton therapy we performed ^{18}F-DOPA and ^{18}F-FDG-PET again that showed the presence of hypercellular and undifferentiated lesions related to change of neoplasm degree (from low to high grade), confirmed by MRS (high Cho peak).

The subsequent surgery demonstrated an astrocytoma grade III WHO (Fig. 9).

Keynotes

Dual-tracer PET imaging may be useful in LLG not only of upgrade diagnosis but in some cases also in differential diagnosis of progression disease versus radiation necrosis.

The ^{18}F-DOPA uptake is related to the prognosis but in this case is also consistent with neoplasm grading [8].

CASE 10: response assessment during and after (photon and proton) radiotherapy and chemotherapy

A 56-year-old man with glioblastoma (GBM) IV grade WHO, glial fibrillary acidic protein in specimen (GFAP) positive, IDH1 wt (wild type), MGMT mutated, Ki67 (7%), after neurosurgery underwent photon radiotherapy (6000 cGy in 30 fractions). Before photon therapy, ^{18}F-DOPA-PET (A) showed high tracer uptake surrounding the surgical crater in right frontal lobe.

12 months later, a recurrence was suspected, based on contrast-enhancing area on MRI scans. A second ^{18}F-DOPA-PET (B) was acquired, confirming recurrence (significant increase [Delta > 20%] of relative percentage of SUV_{max} Tumor to SUV_{max} Background Ratio—compared to the previous exam) and providing BTV (biological tumor volume) data for protons re-irradiation planning.

Concomitant proton therapy (36 Gy RBE in 18 fractions) and chemotherapy (temozolomide) were performed.

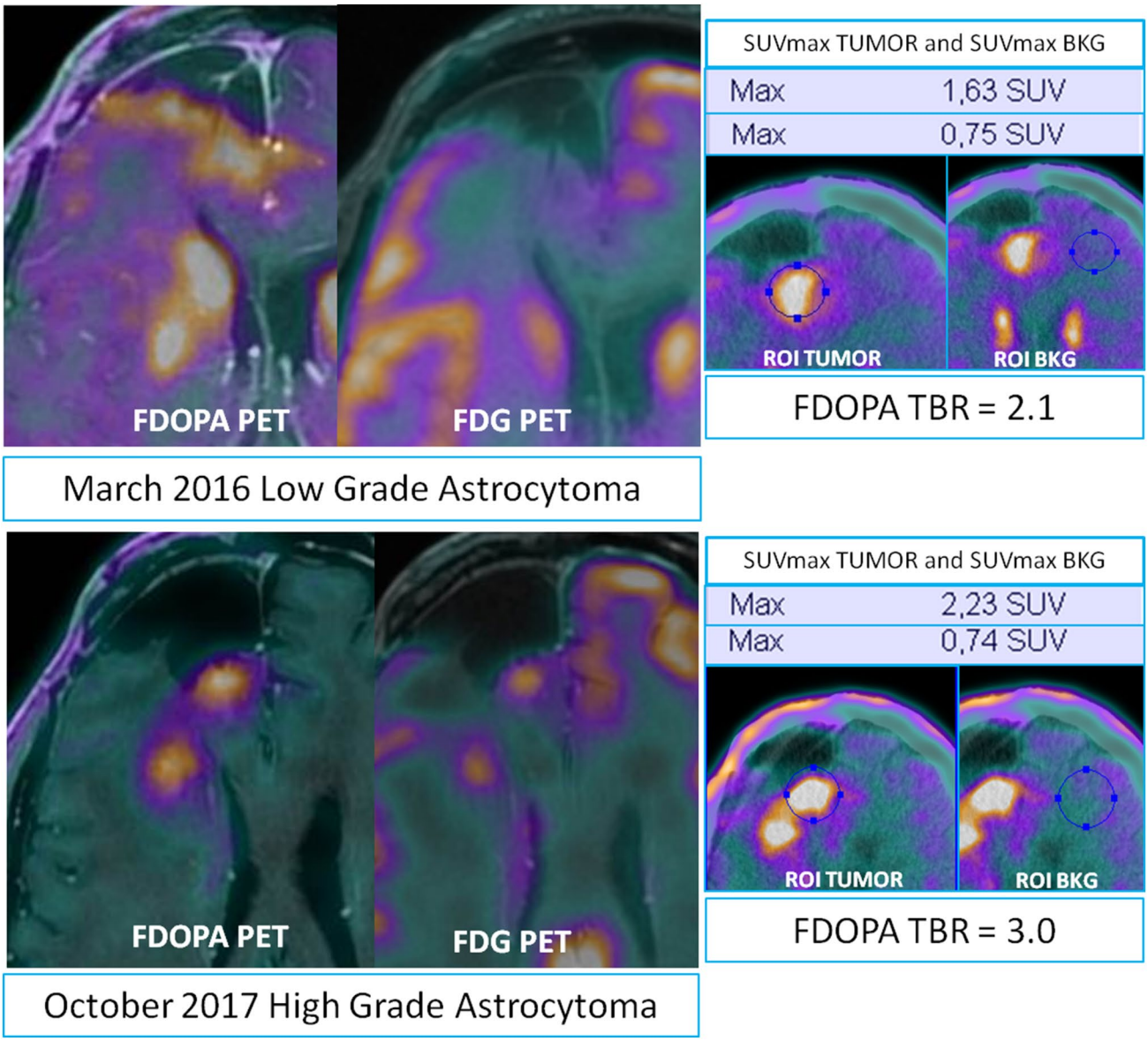

Fig. 9 Disease progression from grades II–III astrocytoma

Repeated ^{18}F-DOPA-PET showed stable uptake values at 8-month follow-up; thereafter, in the PET examination an increased metabolic tumor volume (MTV) was detected exceeding 16% (C). A second-line chemotherapy (fotemustine) was started.

Further ^{18}F-DOPA-PETs showed less tracer lesion uptake and a substantially unchanged MTV, indicative of stable disease. The patient is currently free of disease progression (Fig. 10).

Keynotes

In addition to visual-qualitative assessment, Metabolic Tumor Volume (MTV) may be useful to better assess treatment response. Metabolic findings by PET are helpful in therapy strategy management [34].

Discussions and conclusion

By summarizing the above-mentioned clinical cases, we can suggest the following.

First diagnosis

PET-MR fusion imaging and dynamic ^{18}F-FET or ^{18}F-DOPA-PET must be considered to optimize the diagnosis;

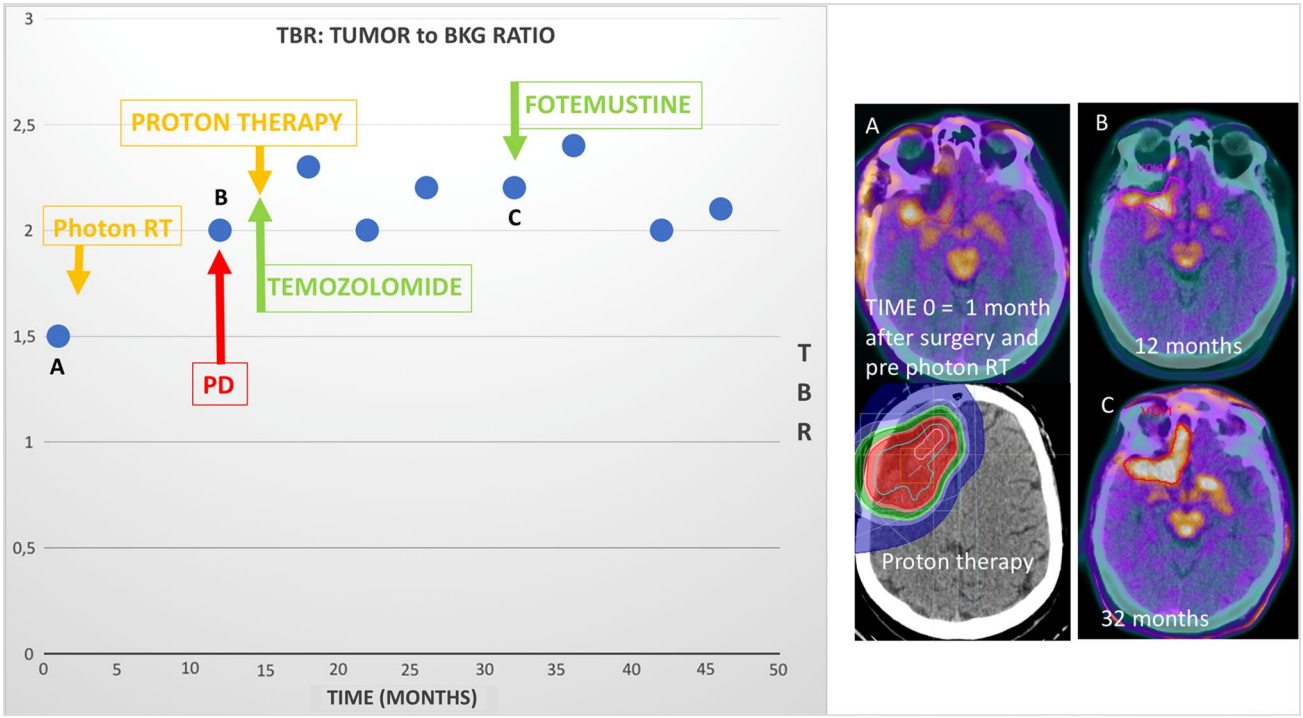

Fig. 10 Response assessment during and after (photon and proton) radio- and chemotherapies. *TBR* tumor to background ratio

Knowledge of all patients' clinical history is mandatory for a correct PET interpretation in the field of differential brain lesion diagnosis;

In case of systemic disease suspicion, the combined evaluation of AA-PET with FDG-PET scans can be useful;

For accurate tumor grading and prognosis, a dynamic FET-PET acquisition is needed, linked to the evidences in time/activity curve;

The morphology of AA-PET uptake area could play an important role in guiding biopsy.

Therapy planning

To detect any disease persistence to be treated with radiotherapy, AA-PET scan can be performed within only 1 month post-neurosurgery;

For radiotherapy planning, the BTV identification has led to a more accurate definition of the target to be treated;

The opportunity to perform a re-irradiation may be supported by the evaluation of MTV as assessed by AA tracer PET;

For recurrence diagnosis it is mandatory to know timing, duration and doses of both recent and previous therapies (radiotherapy, chemotherapy, steroid, antiepileptic, antiangiogenetic, etc.) that can heavily modify the PET data assessment.

Therapy monitoring

During therapy monitoring, AA-PET exams should be performed ≥ 3 months after the end of radiotherapy if radiation necrosis is suspected;

In case of tumor recurrence, the clinical value of AA-PET scan is useful to make the therapeutic decisions.

In conclusion, ^{18}F-FDG and AA-PET imaging is a good tool for brain tumor patient management, but requires implementation of a structured multidisciplinary board (neurosurgery, radiologist, radiotherapist, oncologist and nuclear medicine doctor) to give the best results.

Compliance with ethical standards

Conflict of interest All authors declare that they have no conflict of interest.

Ethical approval All procedures performed in studies involving human participants were in accordance with the ethical standards of the institutional and/or national research committee and with the 1964 Helsinki declaration and its later amendments or comparable ethical standards.

Informed consent Informed consent was obtained from all individual participants included in the study.

References

1. Crocetti E, Trama A, Stiller C, Caldarella A, Soffietti R, Jaal J, Weber DC, Ricardi U, Slowinski J, Brandes A (2012) Epidemiology of glial and non-glial brain tumours in Europe. Eur J Cancer 48(10):1532–1542. https://doi.org/10.1016/j.ejca.2011.12.013 **(Epub 2012 Jan 7)**
2. Linee Guida delle Neoplasie Cerebrali. AIOM (Associazione Italiana Oncologia Medica) Edizione 2017
3. Louis DN, Perry A, Reifenberger G, von Deimling A, Figarella-Branger D, Cavenee WK, Ohgaki H, Wiestler OD, Kleihues P, Ellison DW (2016) The 2016 World Health Organization Classification of tumors of the central nervous system: a summary. Acta Neuropathol. https://doi.org/10.1007/s00401-016-1545-1
4. Essig M, Anzalone N, Combs SE, Dörfler A, Lee SK, Picozzi P, Rovira A, Weller M, Law M (2012) MR imaging of neoplastic central nervous system lesions: review and recommendations for current practice. AJNR 33(5):803–817. https://doi.org/10.3174/ajnr.A2640
5. Al-Okaili RN, Krejza J, Wang S, Woo H, Melhem ER (2006) Advanced MR imaging techniques in the diagnosis of intraaxial brain tumors in adults. Radiographics 26(Suppl 1):S173–S189
6. Thust SC, Heiland S, Falini A, Jäger HR, Waldman AD, Sundgren PC, Godi C, Katsaros VK, Ramos A, Bargallo N, Vernooij MW, Yousry T, Bendszus M, Smits M (2018) Glioma imaging in Europe: a survey of 220 centres and recommendations for best clinical practice. Eur Radiol 28(8):3306–3317
7. Pyka T, Gempt J, Bette S, Ringel F, Förster S (2017) Positron emission tomography and magnetic resonance spectroscopy in cerebral gliomas. Clin Transl Imaging 5(2):151–158
8. Chen W, Silverman DHS, Delaloye S, Czernin J, Kamdar N, Pope W, Satyamurthy N, Schiepers C, Cloughesy T (2006) 18F-FDOPA PET imaging of brain tumors: comparison study with 18F-FDG PET and evaluation of diagnostic accuracy. J Nucl Med 47:904–911
9. Gulyás B, Halldin C (2012) New PET radiopharmaceuticals beyond FDG for brain tumor imaging. Q J Nucl Med Mol Imaging 56(2):173–190
10. A joint RANO/EANO/EANM practice guideline/SNMMI procedure standard for imaging of gliomas using PET with radiolabeled amino acids and [18F]FDG: version 1.0
11. Filss CP, Cicone F, Jon Shah N, Galldiks N, Langen K-J (2017) Amino acid PET and MR perfusion imaging in brain tumours. Clin Transl Imaging 5(3):209–223
12. Oehlke O, Grosu AL (2016) A-L.PET/MRI and brain tumors: focus on radiation oncology treatment planning. Clin Transl Imaging 2(5):159–167
13. Albert NL, Weller M, Suchorska B, Galldiks N, Soffietti R, Kim MM, la Fougère C, Pope W, Law I, Arbizu J, Chamberlain MC, Vogelbaum M, Ellingson BM, Tonn JC (2016) Response Assessment in Neuro-Oncology working group and European Association for Neuro-Oncology recommendations for the clinical use of PET imaging in gliomas. Neuro Oncol 18:1199–1208
14. Jansen NL, Suchorska B, Wenter V, Schmid-Tannwald C, Todica A, Eigenbrod S, Niyazi M, Tonn JC, Bartenstein P, Kreth FW, la Fougère C (2015) Prognostic significance of dynamic 18F-FET PET in newly diagnosed astrocytic high-grade glioma. J Nucl Med 56:9–15
15. Pöpperl G, Kreth FW, Mehrkens JH, Herms J, Seelos K, Koch W, Gildehaus FJ, Kretzschmar HA, Tonn JC, Tatsch K (2007) FET PET for the evaluation of untreated gliomas: correlation of FET uptake and uptake kinetics with tumour grading. Eur J Nucl Med Mol Imaging 34(12):1933–1942
16. Verger A, Stoffels G, Bauer EK, Lohmann P, Blau T, Fink GR, Neumaier B, Shah NJ, Langen K-J, Galldiks N (2018) Static and dynamic 18F-FET PET for the characterization of gliomas defined by IDH and 1p/19q status. Eur J Nucl Med Mol Imaging 45:443–451
17. Fueger BJ, Czernin J, Cloughesy T, Silverman DH, Geist CL, Walter MA, Schiepers C, Nghiemphu P, Lai A, Phelps ME, Chen W (2010) Correlation of 6-18F-fluoro-L-dopa PET uptake with proliferation and tumor grade in newly diagnosed and recurrent gliomas. J Nucl Med 51:1532–1538
18. Bell C, Dowson N, Puttick S, Gal Y, Thomas P, Fay M, Smith J, Rose S (2015) Increasing feasibility and utility of 18F-FDOPA PET for the management of glioma. Nucl Med Biol 42:788–795
19. Pafundi DH, Laack NN, Youland RS, Parney IF, Lowe VJ, Giannini C, Kemp BJ, Grams MP, Morris JM, Hoover JM, Hu LS, Sarkaria JN, Brinkmann DH (2013) Biopsy validation of 18F-DOPA PET and biodistribution in gliomas for neurosurgical planning and radio- therapy target delineation: results of a prospective pilot study. Neuro Oncol 15(8):1058–1067
20. Takahashi Y, Akahane T, Yamamoto D, Nakamura H, Sawa H, Nitta K, Ide W, Hashimoto I, Kamada H (2014) Correlation between positron emission tomography findings and glucose transporter 1, 3 and L-type amino acid transporter 1 mRNA expression in primary central nervous system lymphomas. Mol Clin Oncol 2:525–529
21. Chiavazza C, Pellerino A, Ferrio F, Cistaro A, Soffietti R, Rudà R (2018) Primary CNS lymphomas: challenges in diagnosis and monitoring. BioMed Res Int. https://doi.org/10.1155/2018/3606970
22. Kawai N, Miyake K, Yamamoto Y, Nishiyama Y, Tamiya T (2013) 18F-FDG PET in the diagnosis and treatment of primary central nervous system lymphoma. BioMed Res Int. https://doi.org/10.1155/2013/247152
23. Maza S, Buchert R, Brenner W, Munz DL, Thiel E, Korfel A, Kiewe P (2013) Brain and whole-body FDG-PET in diagnosis, treatment monitoring and long-term follow-up of primary CNS lymphoma. Radiol Oncol 47(2):103–110
24. Dadone-Montaudié B, Ambrosetti D, Dufour M, Darcourt J, Almairac F, Coyne J, Virolle T, Humbert O, Burel-Vandenbros F (2017) [18F] FDOPA standardized uptake values of brain tumors are not exclusively dependent on LAT1 expression. PLoS One 22 12(9):e0184625. https://doi.org/10.1371/journal.pone.0184625
25. Freyschlag CF, Krieg SM, Kerschbaumer J, Pinggera D, Forster MT, Cordier D, Rossi M, Miceli G, Roux A, Reyes A, Sarubbo S, Smits A, Sierpowska J, Robe PA, Rutten GJ, Santarius T, Matys T, Zanello M, Almairac F, Mondot L, Jakola AS, Zetterling M, Rofes A, von Campe G, Guillevin R, Bagatto D, Lubrano V, Rapp M, Goodden J, De Witt Hamer PC, Pallud J, Bello L, Thomé C, Duffau H, Mandonnet E (2018) Imaging practice in low-grade gliomas among European specialized centers and proposal for a minimum core of imaging. J Neurooncol 139:699–711. https://doi.org/10.1007/s11060-018-2916-3
26. Cendes F, Theodore WH, Brinkmann BH, Sulc V, Cascino GD (2016) Neuroimaging of epilepsy. Handb Clin Neurol 136:985–1014
27. Lupo JM, Nelson SJ (2014) Advanced MR imaging methods for planning and monitoring radiation therapy in patients with high grade glioma. Semin Radiat Oncol 24(4):248–258
28. Walker J, Ruzevick J, Malayeri AA, Rigamonti D, Lim M, Redmond KJ, Kleinberg L (2014) Postradiation imaging changes in the CNS: how can we differentiate between treatment effect and disease progression? Future Oncol 10(7):1277–1297
29. Herrmann K, Czernin J, Cloughesy T, Lai A, Pomykala L, Benz MR, Ak Buck, Phelps ME, Chen W (2014) Comparison of visual and semiquantitative analysis of 18F-FDOPA-PET/CT for recurrence detection in glioblastoma patients. Neuro Oncol 16:603–609
30. Hatzoglou V, Ulaner GA, Zhang Z, Beal K, Holodny AI, Young RJ (2013) Comparison of the effectiveness of MRI perfusion and

fluorine-18 FDG PET-CT for differentiating radiation injury from viable brain tumor. Clin Imaging 37(3):451–457
31. Miller-Thomas MM, Benzinger TLS (2017) Neurological applications of PET/MR. Magn Reson Imaging Clin N Am 25(2):297–313
32. Toch SR, Poussier S, Micard E, Bertaux M, Van Der Gucht A, Chevalier E, Marie PY, Guedj E, Verger A (2018) Physiological whole-brain distribution of [18F]FDOPA uptake index in relation to age and gender: results from a voxel-based semi-quantitative analysis. Mol Imaging Biol. https://doi.org/10.1007/s11307-018-1256-1
33. Chen W (2007) Clinical applications of PET in brain tumors. J Nucl Med 48:1468–1481
34. Lizarraga KJ, Allen-Auerbach M, Czernin J, DeSalles AAF, Yong WH, Phelps ME, Chen W (2014) 18F-FDOPA PET for differentiating recurrent or progressive brain metastatic tumors from late or delayed radiation injury after radiation treatment. J Nucl Med 55:1–7